

Supporting Information

Dendrite-free and air-stable lithium metal batteries enabled by electroless plating with aluminum fluoride

Zaisheng Wang,^{a†} Zhenming Xu,^{d†} Xiaojing Jin,^a Jianhui Li,^c Qingshuai Xu,^a Yanan

Chong,^a Weishan Li,^c Daiqi Ye,^a Yingying Lu,^e Yongcai Qiu^{a,b*}

^a School of Environment and Energy, South China University of Technology,
Guangzhou 510006, China

^b State Key Laboratory of Luminescent Materials and Devices, South China
University of Technology, Guangzhou, China

^c School of Chemistry and Environment, South China normal University, Guangzhou
510006, China

^d Harvard John. A. Paulson School of Engineering and Applied Sciences, Harvard
University, 29 Oxford St, Cambridge, Massachusetts, 02138, USA

† These authors contributed equally to this work.

*Corresponding Author E-mail: (ycqiu@scut.edu.cn;)

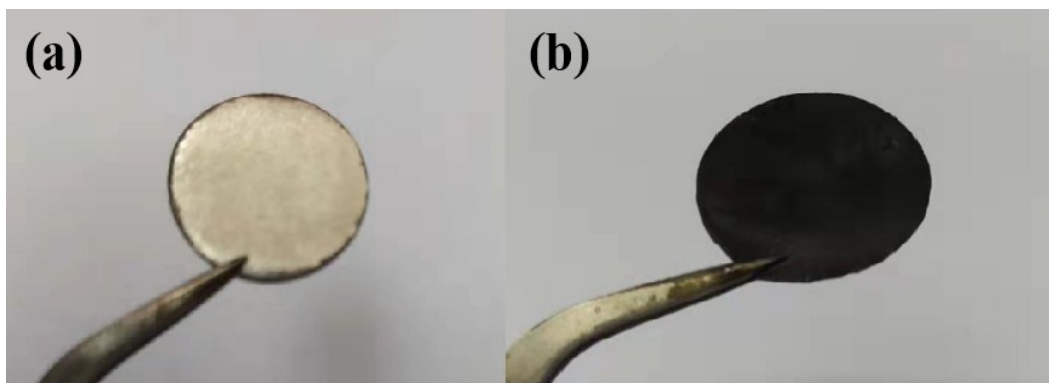


Figure S1. Digital photos of (a) Li foil and (b) Li surface after reacting with a supersaturated solution of AlF_3 in carbonate ester electrolyte.

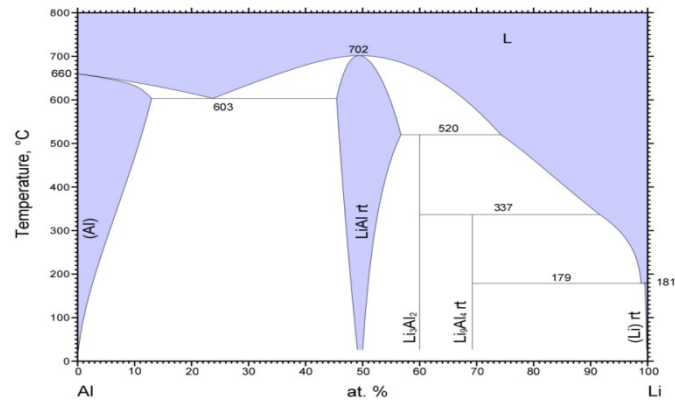


Figure S2. Phase diagram of Li with Al. L refers to liquid, whereas Li means lithium metal phase at room temperature.

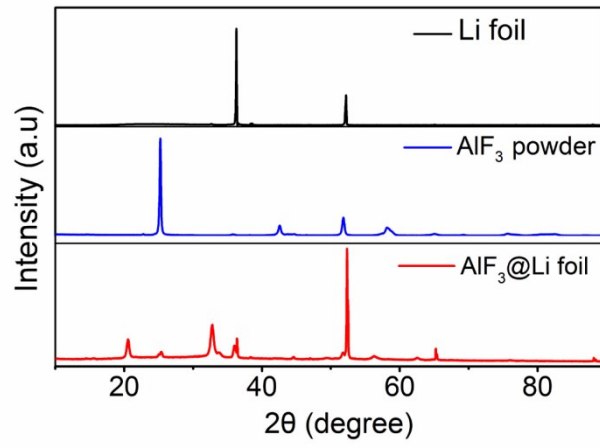


Figure S3. XRD characterizations of Li foil, AlF₃ powder and AlF₃@Li foil.

Surface	eV/Å ²
001	0.155
010	0.096
011	0.122
012	0.117
021	0.121
100	0.080
101	0.099
102	0.126
110	0.107
111	0.105
112	0.116
120	0.107
121	0.121
201	0.110
210	0.112
211	0.123

Table S1. DFT calculated surface energies of the low-index surfaces of Li₉Al₄ alloy.

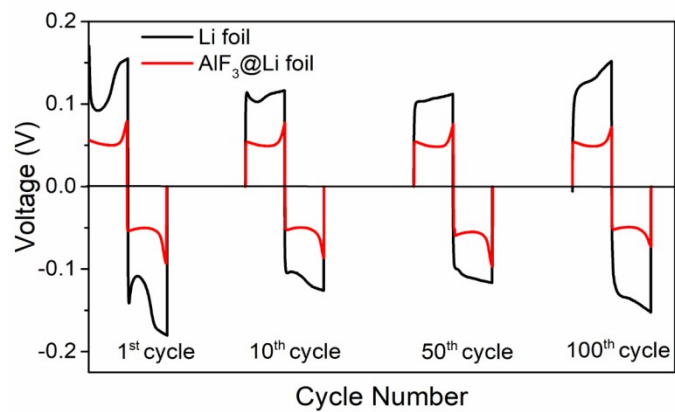


Figure S4. Voltage profile of Li foil and AlF₃ protected symmetric cell during the 1st, 10th, 50th and 100th cycle, with a current density of 1 mA cm⁻².

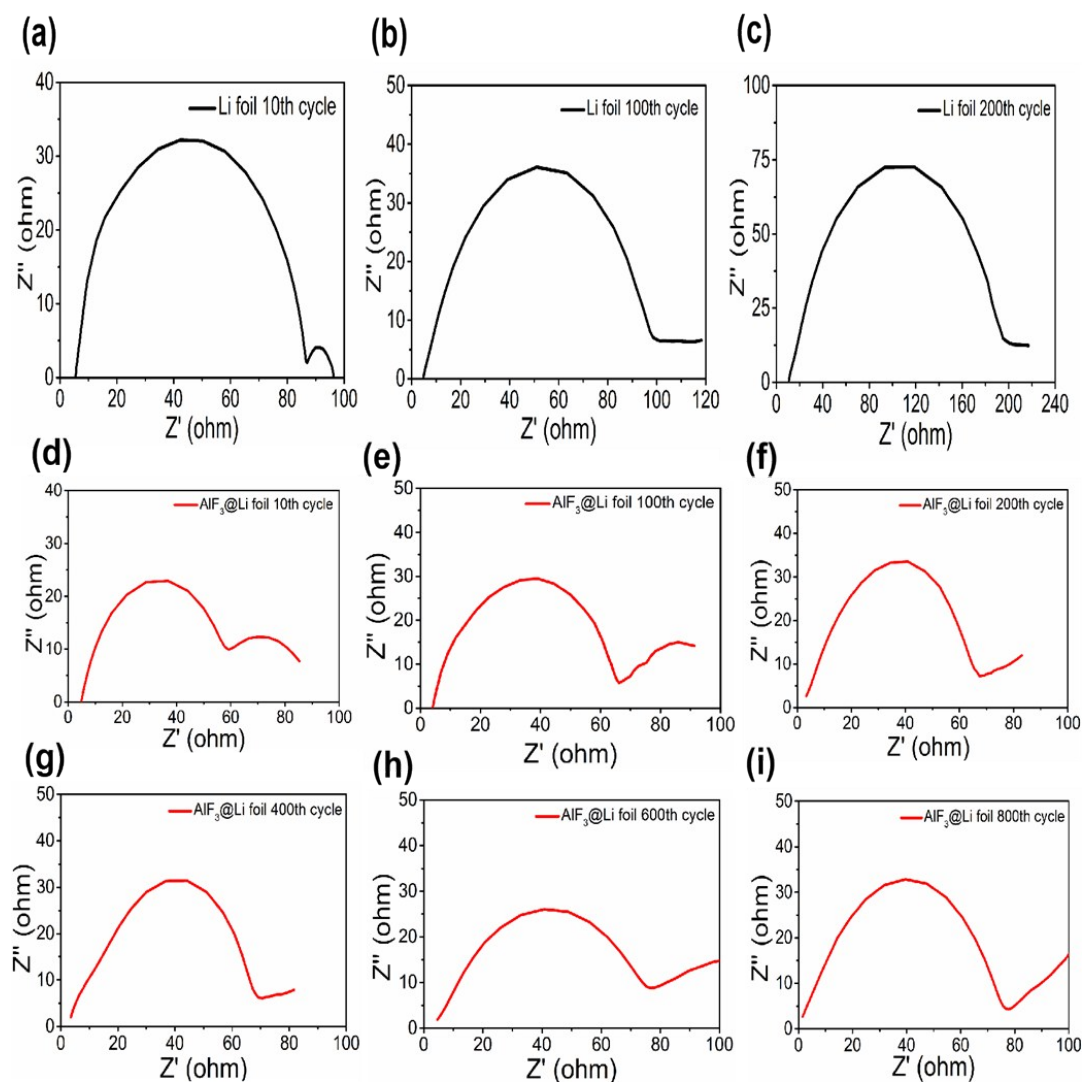


Figure S5. Electrochemical impedance spectra (EIS) of the symmetric cells at different cycle for Li foil (black), $\text{AlF}_3@Li$ foil (red).

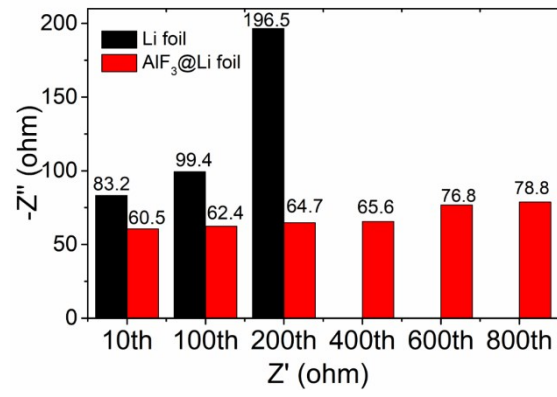


Figure S6. EIS comparison of symmetric cells after 10, 100, 200, 400, 600 and 800 cycles.

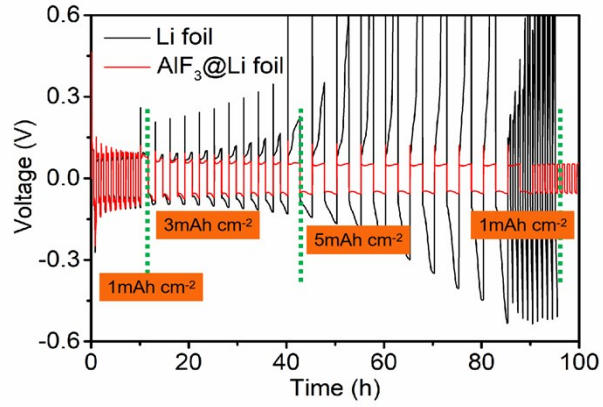


Figure S7. Symmetric cell cycling performance comparison between Li foil (black), AlF₃@Li foil (red) film under different areal capacity from 1 to 5 mAh cm⁻². Current density was fixed at 1 mA cm⁻².

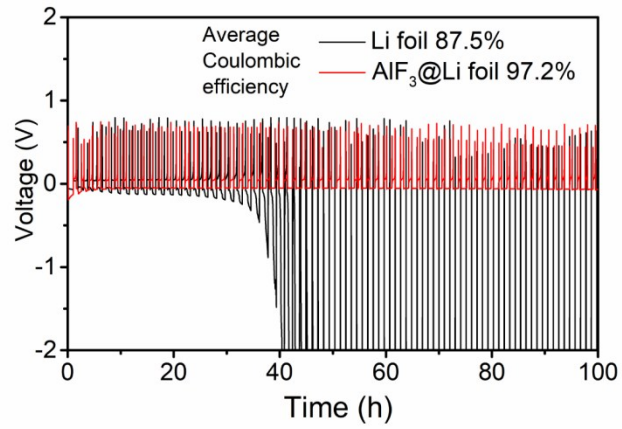


Figure S8. Voltage-time curves to calculate the average coulombic efficiency of the pre-plated 3.0 mAh cm^{-2} Li for the Li foil and $\text{AlF}_3@\text{Li}$ foil at a current density of 1 mA cm^{-2} (1 mAh cm^{-2} capacity).

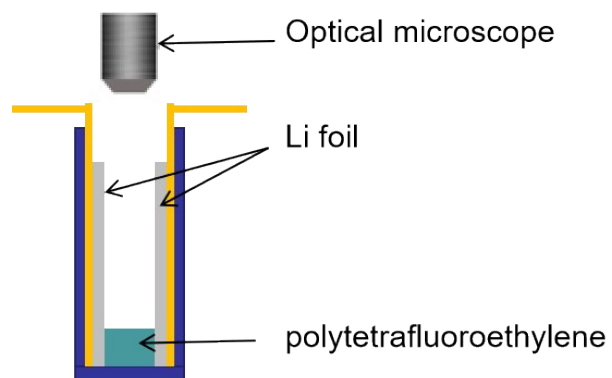


Figure S9. Operando optical microscopy adopted to investigate *in-situ* Li plating behavior.

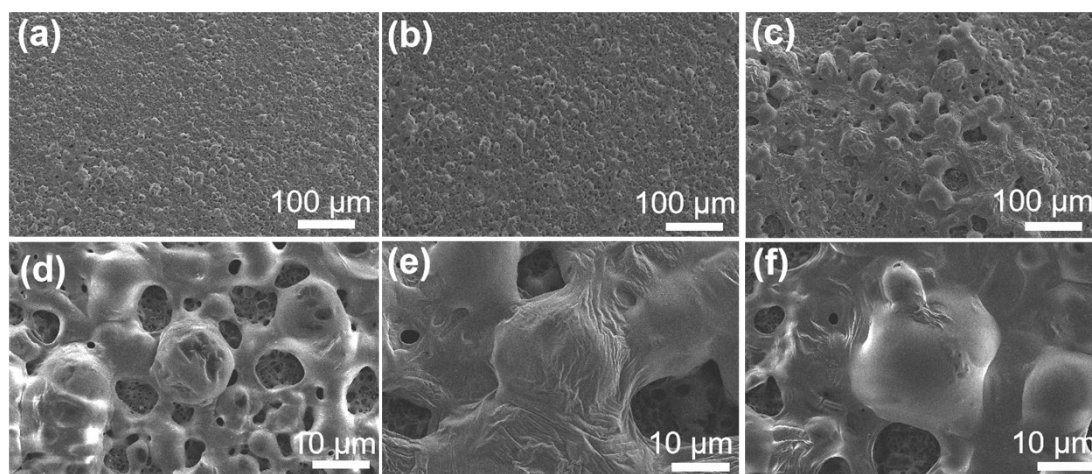


Figure S10. SEM of Li deposits on AlF_3 protected Li foil. (a and d) 0.1 mAh cm^{-2} , (b and e) 0.5 mAh cm^{-2} , and (c and f) 1 mAh cm^{-2} . Current density, $J = 1 \text{ mAh cm}^{-2}$.

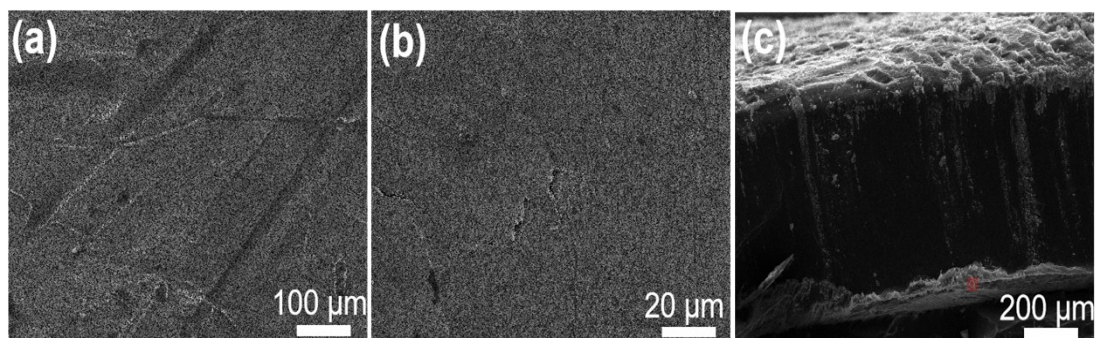


Figure S11. Top-view (a, b) and cross-sectional (c) SEM images of Li foil electrode before cycling.

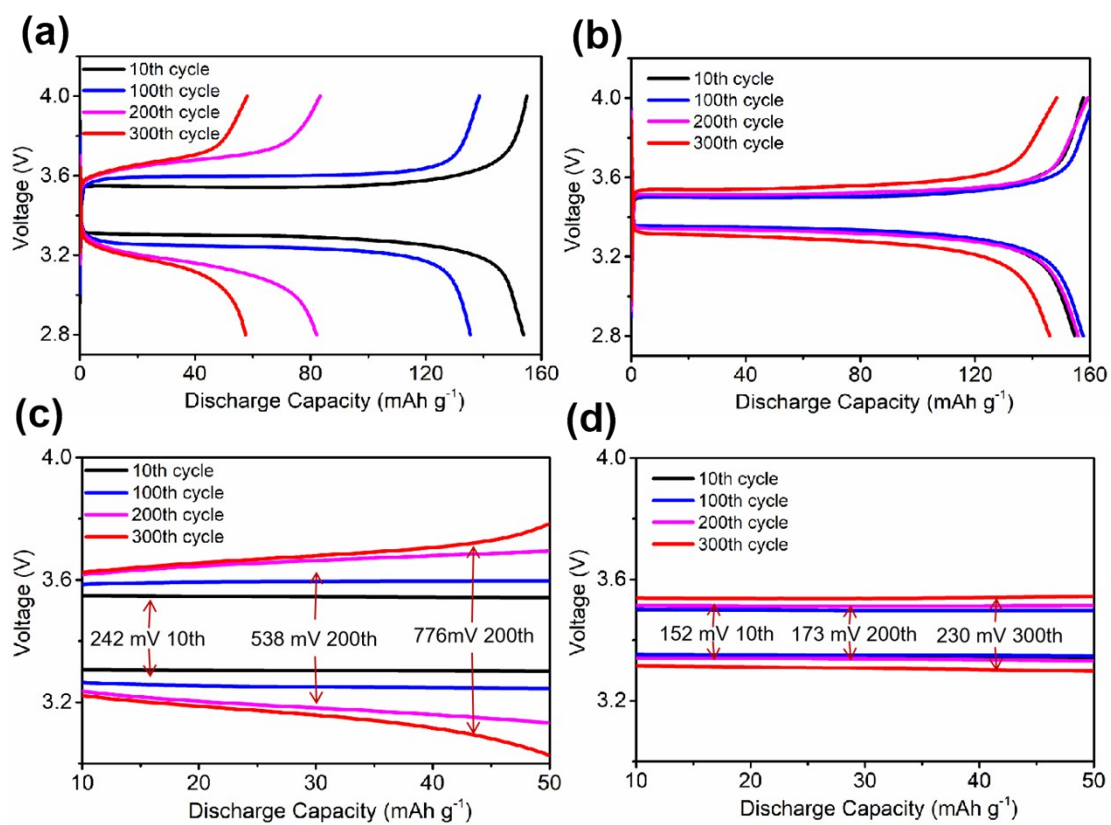


Figure S12. The selected (a, b) voltage capacity curves and (c, d) voltage hysteresis of Li foil (a, c) and AlF₃ protected Li foil cells (c, d) in the long term cycles at a rate of 1C (1C=160 mA g⁻¹).

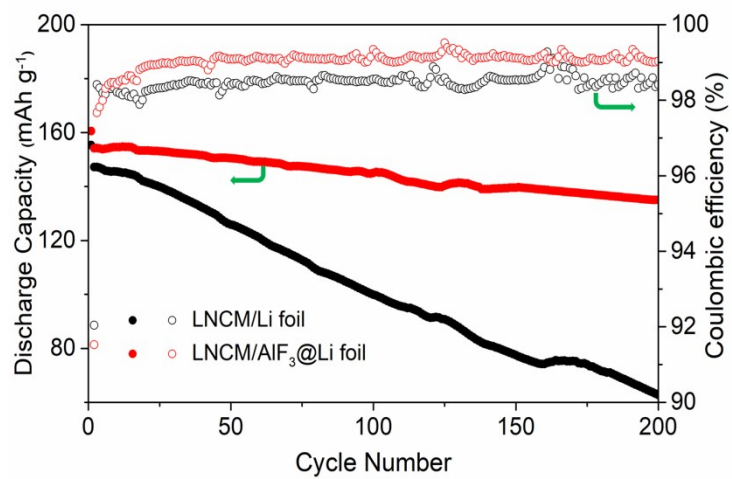


Figure S13. Cyclic stability of Li-LNCM battery at 0.5 C rate with high mass loading (6 mg cm⁻², 1.1 mAh cm⁻²) in the voltage range from 3 to 4.3 V (vs. Li/Li⁺).

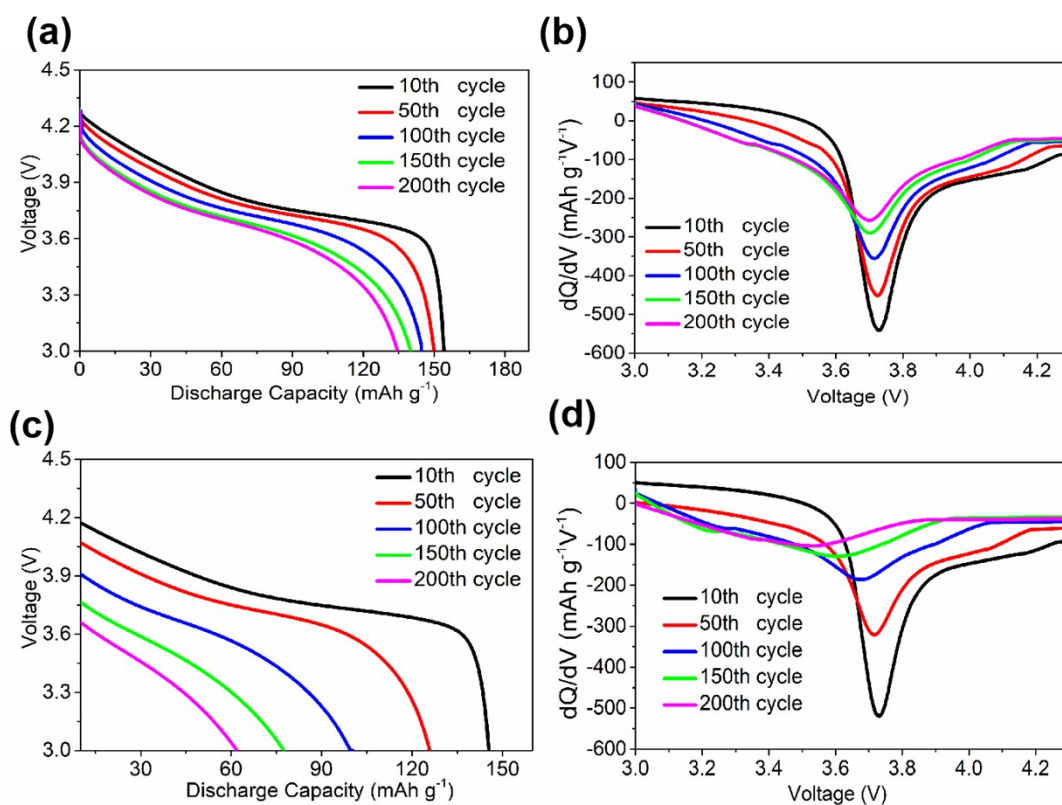


Figure S14. Electrochemical performance of rechargeable lithium metal batteries. (a and c) Discharge capacity curves of the Li foil and AlF₃ protected Li anode of Li-LNCM batteries at 0.5 C rate. (b and d) Differential discharge capacity curves of the Li foil and AlF₃ protected Li anode cell of Li-LNCM batteries at 0.5 C rate. The evolution of peak intensities with the increasing of the cycling times reveals that the protected layer can significantly improve the interface stability between electrolyte and Li foil.

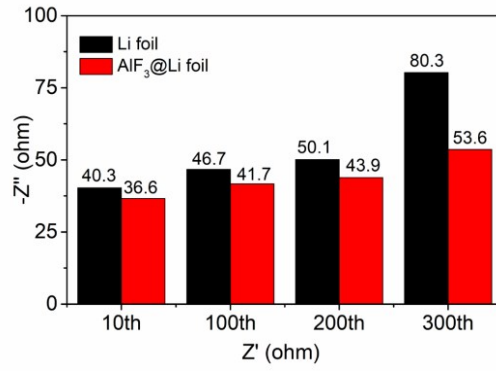


Figure S15. EIS comparison of Li-LFP batteries after 10, 100, 200 and 300 at 1 C rate.

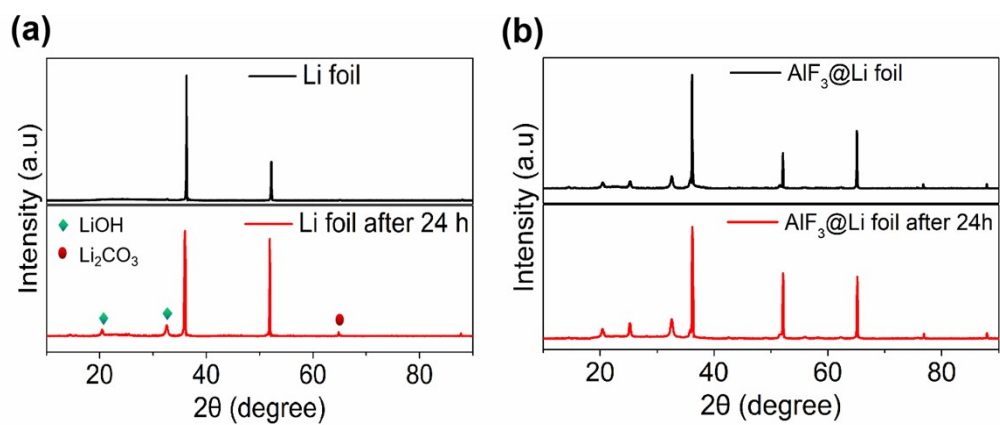


Figure S16. XRD characterization of Li foil (a) and AlF₃ protected Li foil (b) before and after 24 h exposed to air at 25°C and 25% humidity.

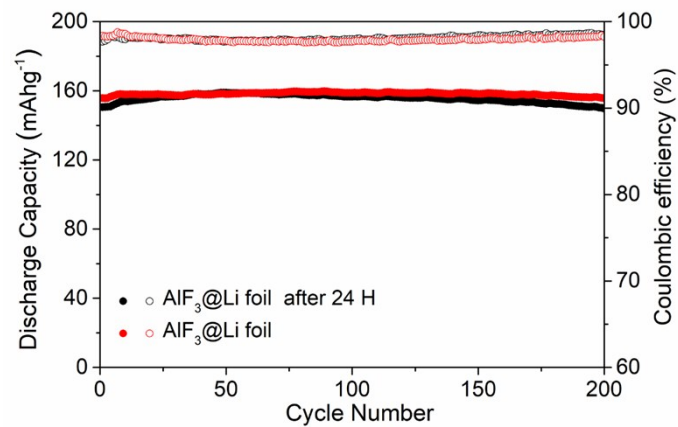


Figure S17. Cycling performance of Li-LFP batteries at 1 C rate in voltage range from 2.8 to 4.0 V using AlF_3 protected Li foil before and after exposure to air at 25°C and 25% relative humidity for 24 h.

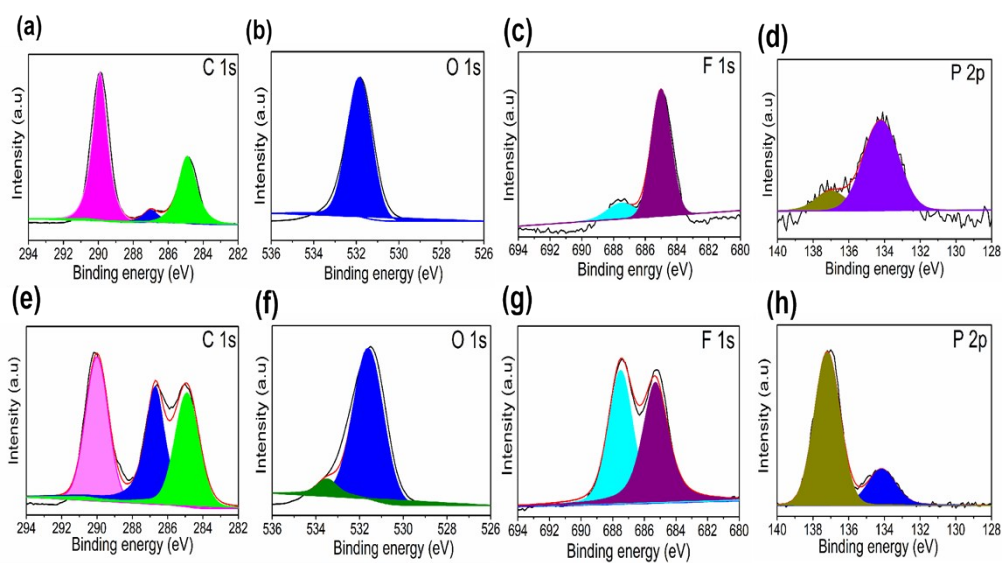


Figure S18. Surface chemistry of Li metal anode before (a-d) and after (e-h) 100 cycles. X-ray photoelectron spectroscopy (XPS) of (a. e) C 1s; (b. f) O 1s; (c. g) F 1s; (d. h) P 2p.

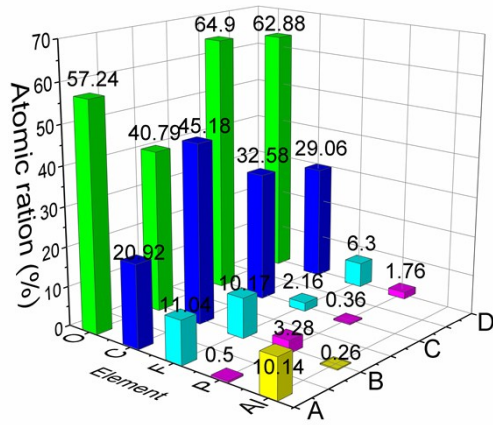


Figure S19. Surface chemistry of Li metal anode. The comparison of various element atoms content ratio of the AlF_3 protected Li (A. B) and Li foil (C. D) before (A. C) and after 100 (B. D) cycles.